the tropical Atlantic Ocean

SABINE ARNAULT,* LIONEL GOURDEAU† and YVES MENARD†

Abstract—An intensive survey of XBT and surface salinity sampling was carried out during September/October 1988 to compare surface dynamic height anomalies and altimetric anomalies along a line close to a GEOSAT satellite track in the Tropical Atlantic Ocean, 15°N–18°S. Hydrography and altimetry agree within 4 cm rms, except in the southern part of the section (south of 5°S). In the northern hemisphere, the correlation between the two data sets is about 0.80 and the two power spectra present the same energy level, with a k^{-1}–k^{-2} dependence. The hydrographic data show an unusual tongue of fresh water around 7°N that results in positive dynamic height anomalies of about 10 dyn cm. The GEOSAT data analysed during the same period also show these anomalies with a similar scale.

1. INTRODUCTION

RADAR altimeter observation of the sea surface has proved a powerful means of acquiring synoptic scale data for a variety of ocean phenomena. CHENEY and MARSH (1981) used SEASAT altimeter data to map the Gulf Stream and rings in the western North Atlantic. By using SEASAT data, MÉNARD (1983) observed high variability of the sea surface topography (up to 20 cm) in the vicinity of the Gulf Stream and Kuroshio, and FU and CHELTON (1985) and DANIAULT and MÉNARD (1985) showed a large-scale coherence in the temporal variability of the Antarctic Circumpolar Current. More recently, using the GEOSAT altimeter data, TAI et al. (1989) generated a sea-level time series and found approximately 4 cm rms agreement with Pacific island tide gauges. CHENEY et al. (1989) confirmed this conclusion by finding an agreement less than 4 cm rms. KOSRO et al. (1988) obtained similar results in comparing GEOSAT collinear profiles with repeated hydrographic sections along the California coast.

These results were based on available ship and *in situ* data collected for purposes other than comparison with altimeter data. Most of the available *in situ* data miss the close temporal and spatial coincidence with the altimeter data. When comparing with tide gauge time series, the principal question is whether sea level measured at an isolated point on an island accurately represents sea level in the surrounding open ocean. For this reason, a specific experiment was needed.

*LODYC/ORSTOM, UPMC T14-2, 4 place Jussieu, 75252 Paris Cedex 05, France.
†CNES/GRGS, 18 ave E. Belin, 31055 Toulouse Cedex, France.

- 3 AOUT 1995

BERNSTEIN *et al.* (1982) compared the dynamic height changes from repeated tracks of SEASAT altimeter data with data obtained from aircraft AXBTs across the Kuroshio extension. The two data sets agree generally within 10 cm for surface height changes due to the time-varying geostrophic current. Nevertheless, a time shift of about 1 day was present between the *in situ* and the satellite data. We report in this paper a similar experiment using GEOSAT altimeter data and XBTs launched from a ship crossing the tropical Atlantic ocean.

Knowledge of the tropical ocean circulation is essential when considering climate problems. The most striking and well known examples of correlation between climatic events and ocean tropical circulation are found in the Pacific, especially during El Nino events. However, because of its smaller size, the seasonal wind patterns and its meridional heat transport cross the Equator (HASTENRATH, 1982), study of the tropical Atlantic is also interesting with respect to tropical circulation.

Despite large oceanographic experiments carried out in recent years (FOCAL/ SEQUAL, 1982–1984), the basinwide data coverage of the tropical Atlantic is still poor. Satellite data, such as altimeter data, can help solve this problem. MÉNARD (1988) and ARNAULT *et al.* (1990) have shown the good consistency of the large-scale seasonal variability of the tropical Atlantic as observed by altimeter data with respect to climatology and models. However, compared to the large dynamic topography signal across the Gulf Stream and Kuroshio regions, the tropical Atlantic presents only a 10 cm signal so that the differences between *in situ* data and altimetry are difficult to analyse. Thus, the validation of altimetry in the tropical regions requires careful investigation.

2. THE ARAMIS 1 EXPERIMENT

Launched in March 1985, the U.S. Navy GEOSAT altimeter performed a geodetic mission during its first 18 months of operation on a non-repeat orbit. In November 1986, it shifted to a 17.05 day repeat orbit. The resolution at the equator is approximately 150 km, and 3 days separate two adjacent tracks. The 1-s alongtrack average computed by CHENEY *et al.* (1987) yields one point every 6.8 km.

Fortunately, one GEOSAT track is practically superimposed on a merchant route from Le Havre, France to Buenos Aires, Argentina. Thus, we organized a cruise on the merchant ship *La Fayette* starting from Le Havre and ending in Buenos Aires: the ARAMIS 1 (Altimétrie sur un Rail Atlantique et Mesures In-Situ) experiment. The aim of this cruise was to perform an intensive launch of XBTs and surface salinity sampling as the satellite was passing over the ship.

The ship left Le Havre on 25 September 1988 and arrived at Buenos Aires on 4 October 1988. The overpass occurred on 2 October, when the ship was located at 3°40'S. About 300 XBTs were launched between 40°N and 20°S. About 200 sea surface salinity samples were taken at the same time. The distance between two temperature measurements decreased from 180 km north of 20°N to about 2 km near the Equator (Fig. 1).

3. DATA PROCESSING AND METHOD

Altimetric data

The altimeter measures the distance from the spacecraft to the ocean. The orbit of the spacecraft is determined by independent ground tracking. Thus, the difference between

the altimeter measurement and the orbit primarily indicates large permanent undulations of the geoid. Superimposed on the geoid undulations are the generally much weaker fluctuations associated with ocean tides and currents. Variability associated with the permanent ocean currents in the tropical Atlantic region is less than 0.1 m (see Fig. 6 of MERLE and ARNAULT, 1985). Differences in measurements made along repeated tracks cannot be due to time-invariant geoid or mean currents, but must be ascribed to time-variable phenomenon such as ocean currents and tides. If attention is paid to spatial length scales less than 1000 km, typical of tropical currents, the large-scale height variability caused by tides as well as the error introduced by uncertainties in the satellite ephemeris can be ignored, leaving time-variable ocean currents as the main source of fluctuations observed by altimetry (BERNSTEIN *et al.*, 1982).

The GEOSAT data set consists of repetitive tracks of 22 passes, from November 1986 to November 1987, plus two cycles during the experiment in September/October 1988. These tracks are numbered from east to west. Track 104 coincides almost perfectly with the shiptrack (Fig. 1). As noted in the GDR GEOSAT handbook (CHENEY *et al.*, 1987), several corrections, which are available with the GDR, have to be applied to the rough
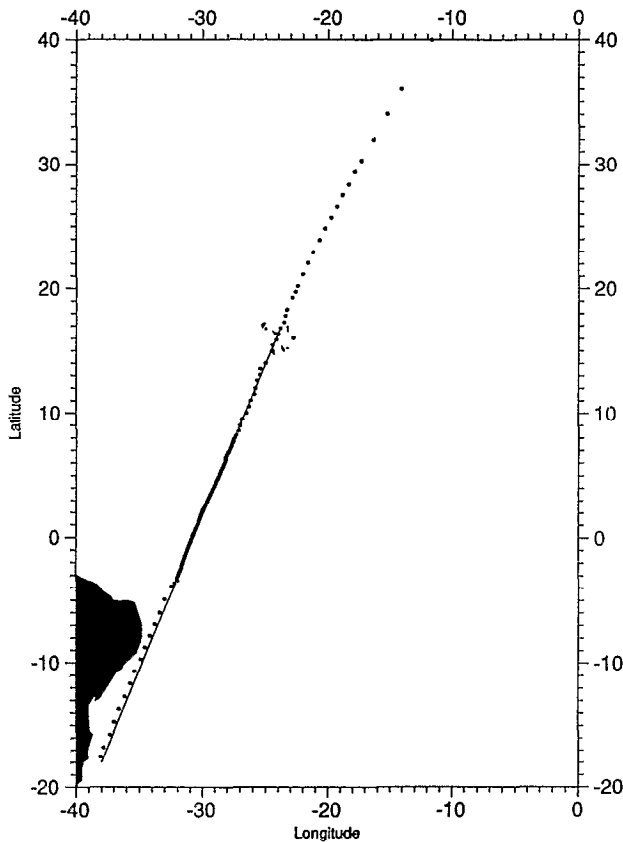

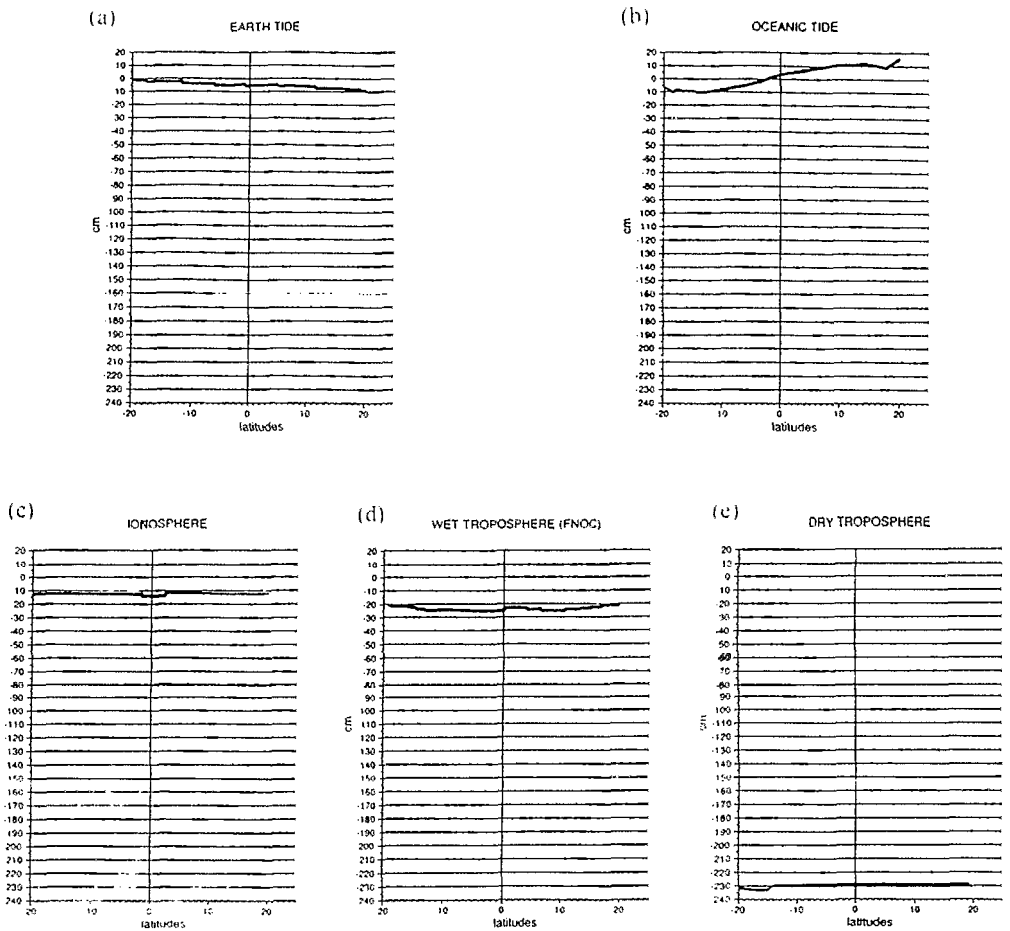Fig. 1. XBT and surface salinity samples along the shiptrack together with the GEOSAT track 104.

Fig. 2. Solid tide (a), ocean tide (b), ionospheric (c), wet tropospheric (d) and dry tropospheric (e) corrections applied to altimetric data.

altimetric data: the largest single source of error in GEOSAT satellite altimeter data is due to the uncertainty of satellite altitude. However, a long wavelength error similar to the SEASAT error can be modelled successfully by a low-degree polynomial. The solid tide was removed according to the model of CARTWRIGHT and TAYLOR (1971) and CARTWRIGHT and EDDEN (1973). The ocean tide was removed using the model of SCHWIDERSKI (1980). Values for these corrections are typically 10 cm (Fig. 2a, b). The error of the solid tide model is unlikely to exceed 1 cm. The ocean tide error is estimated to be 1 cm in the deep sea, but much larger errors can occur near land. Nevertheless, these very long wavelength errors can be eliminated by the adjustment used to remove orbit error. Ionospheric corrections were based on The Global Positioning System climatic ionosphere model. This correction compensates for the altimeter travel time delay caused by free electrons in the ionosphere. The ionosphere model is a simple global scale version driven by daily values of solar flux. Its accuracy is 50% level or better. Values of the correction are typically of the order of 10 cm (Fig. 2c).

Wet and dry tropospheric corrections were applied using the FNOC model (SAASTAMOI-NEN, 1972; TAPLEY *et al.*, 1982). The wet troposphere correction compensates for the altimeter travel time-delay caused by water vapour in the troposphere. The dry troposphere correction compensates for the altimeter travel time delay caused by air molecules in the troposphere. The most questionable of all the GEOSAT corrections is the wet troposphere effect. Several studies showing comparisons between various tropospheric correction models (MONALDO, 1990; JOURDAN *et al.*, 1990) have emphasized that errors of a few centimetres can be unresolved by the FNOC model. In the future, new SSM/I based corrections will allow a more effective reduction of these error sources (EMERY *et al.*, 1990). The dry troposphere correction is better known than the wet troposphere correction, and errors can be largely eliminated by a first degree polynomial adjustment (Fig. 2d, e).

To eliminate spikes in the data, each sampled point (rate: 6.8 km) was compared to a mean sea surface height (MARSH, 1982). If the difference was greater than several metres (depending on the area), the point was flagged.

As noted earlier, the geoid undulations can be removed from the corrected altimetric data by looking at temporal variability. There are three different methods to extract the variability signal from the altimetric data. Crossover differences have given encouraging results in the Tropical Pacific (MILLER *et al.*, 1986). A second method is based on the use of a mean sea surface. MÉNARD (1988) found good agreement between the seasonal variability of the dynamic topography as observed from historical hydrographic data (MERLE and ARNAULT, 1985) and from GEOS 3 and SEASAT altimetric data referred to a mean sea surface. The third one, the collinear profile method we used here, was previously tested with success in a mesoscale study of the northwest Atlantic (MÉNARD, 1983) and in the Pacific (CHENEY *et al.*, 1983; MUSMAN, 1986; MALARDE *et al.*, 1987). This analysis includes the following steps:

(1) The altimetric measurements of the sea surface are resampled along the track at a 10 km spacing, from 20°N to 20°S, using a cubic spline to provide regular sampling.

(2) A first-degree polynomial is fitted to the profiles, and the mean polynomial over the different cycles is added back to each individual adjusted profiles.

(3) The mean profile is then calculated using the average of all the cycles.

(4) The mean profile is subtracted from each individual profile to produce sea level anomalies.

(5) The sea level anomalies are adjusted with a first degree polynomial least-squares fit to absorb long wavelength errors. A final smoothing is performed using a filter over 60 km.

Step 1 provides collocated measurement points for successive passes on the track. Step 2 reduces the possible influence of orbit error on the mean profile because of missing points. Step 3 provides the mean sea surface along the track. Step 4 and step 5 give the sea level anomaly all along the track, sampled every 10 km.

In situ *data*

Traditionally, dynamic height computation requires knowledge of the vertical profiles of temperature and salinity and can be performed only when data are available from a salinity–temperature–depth Z(CTD) record. But, in many regions of the ocean, the relationship between temperature and salinity (T–S) is generally consistent with time. Where such a relationship exists, temperature data alone can be used to compute dynamic

height. The idea of using BT data and a $T–S$ relationship to supplement hydrographic data is not a new one. As early as 1947, STOMMEL explored this hypothesis. EMERY (1975) and EMERY and WERT (1976), using this method in the Pacific, concluded that $T–S$ curves can be used to reliably compute dynamic height from temperature profiles. In the tropical Atlantic, MERLE and ARNAULT (1985) found that the total error on the monthly 0/500 dbar dynamic height computed through a mean $T–S$ relationship is about 2 dyn cm. We therefore used this method in the present study.

About 300 "deep-blue" sippican XBTs launched during the cruise, between 40°N and 20°S, provided a temperature profile up to 700–800 m depth. The use of deeper sounds, which requires low ship speed, was impossible in the case of a merchant ship. All the XBTs were carefully checked to eliminate malfunctions or errors. After this validation and limitation to the tropical region, 253 temperature profiles were kept (Fig. 1). During the same cruise, we also collected 204 surface salinities.

To obtain a mean temporal dynamic height profile along the shiptrack, so that we could compute dynamic height variability, we also used XBTs collected from November 1986 to November 1987, during the TOGA program. Various screening routines were applied to eliminate suspicious or redundant data or profiles that did not reach 500 m. The resulting 86–87 XBTs file contains about 400 temperature profiles.

Monthly climatological $T–S$ relations were computed along the shiptrack using an historical Nansen data set of 1150 $T–S$ profiles (MERLE and ARNAULT, 1985). These data were grouped in large boxes of 8° longitude by 2° latitude. A weighted interpolation from adjacent squares and months has been applied in order to reduce the noise level in squares with scanty or no data.

These monthly $T–S$ were used to compute the mean 86–87 dynamic heights with the 86–87 XBTs file using a salinity interpolation as described above. Then, these monthly climatological mean $T–S$ were adjusted at the surface by the $T–S$ samples taken during ARAMIS 1. These new $T–S$ relationships were used together with the ARAMIS 1 XBTs file to compute the dynamic height during the cruise. The dynamic height anomaly (hereafter DHA) for the cruise—directly comparable with altimetric sea level anomaly (hereafter SLA)—is obtained by subtraction of the mean 86–87 dynamic height. As the total error (including the XBT temperature error of 0.1°C) on the 0/500 dbar dynamic height computed through a mean $T–S$ relationship is less than 2 dyn cm, we assumed the error on the DHA during ARAMIS 1 experiment to be less than 4 dyn cm.

As with the SLA processing, DHA are finally adjusted with a low degree polynom and smoothed using a filter over 60 km.

4. RESULTS

Figure 3 gives the along-shiptrack latitudinal profiles of both the surface temperature (a) and salinity (b) collected during the cruise, compared with historical data. The curves show similar latitudinal variations but with warmer and fresher (less than 33‰) waters around 7°N during the cruise. Usually, surface salinity maps show a large region of fresh water ($S < 36$‰) that extends from the equator to 12°N (DESSIER and DONGUY, 1991). From 1977 to 1986, around 5°N, there were only two salinity values less than 33‰ and four between 34 and 35‰ (DESSIER, personal communication). This observation of extremely low salinities in a narrow region is certainly related to interannual variations as well as the dense sampling of the cruise. Mixing processes also may have been inhibited by unusually weak
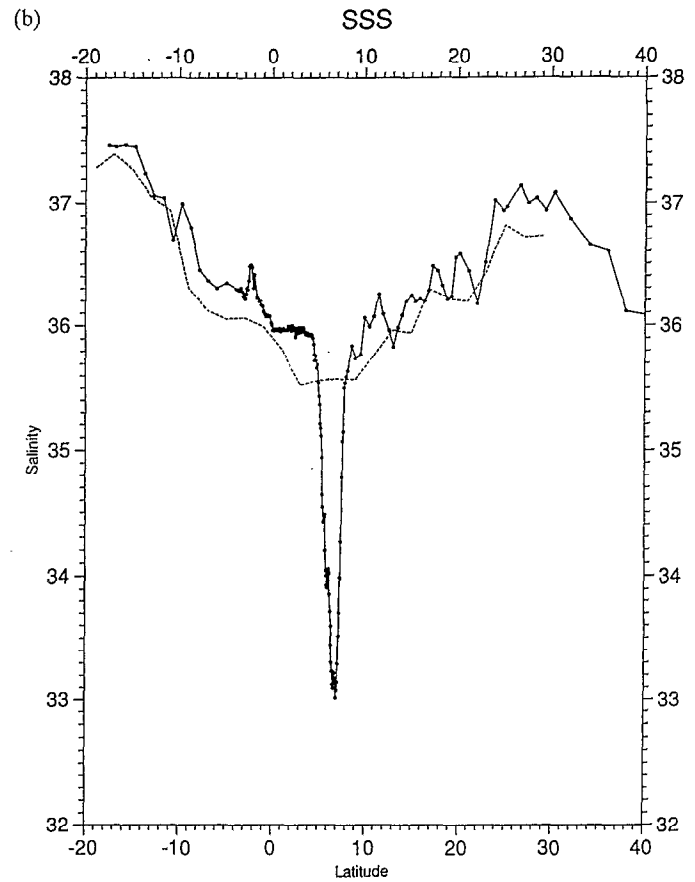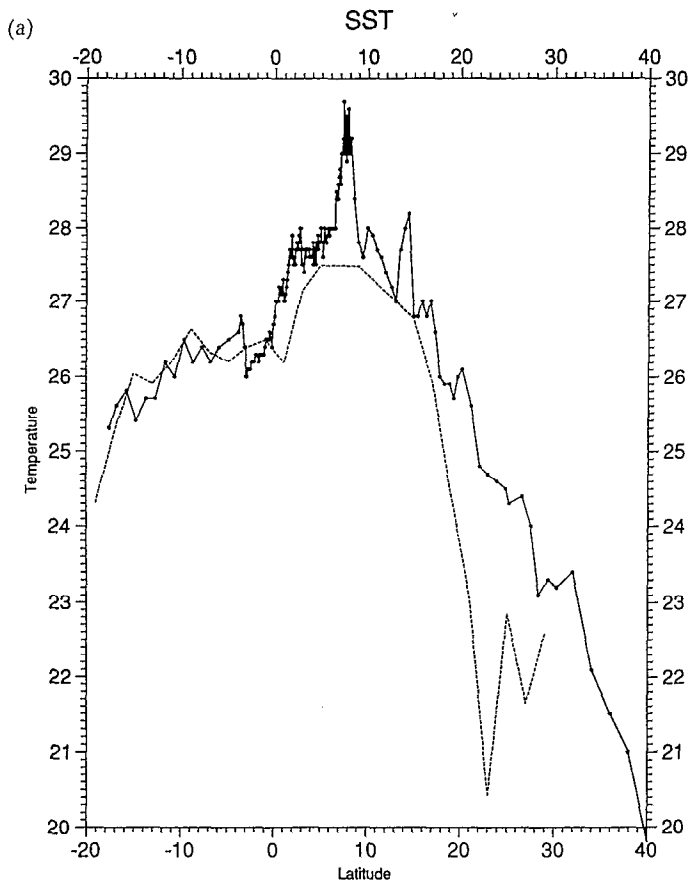
Fig. 3. Observed surface temperature (a) and salinity (b) signals along the shiptrack (solid line) compared with historical data (dashed line).
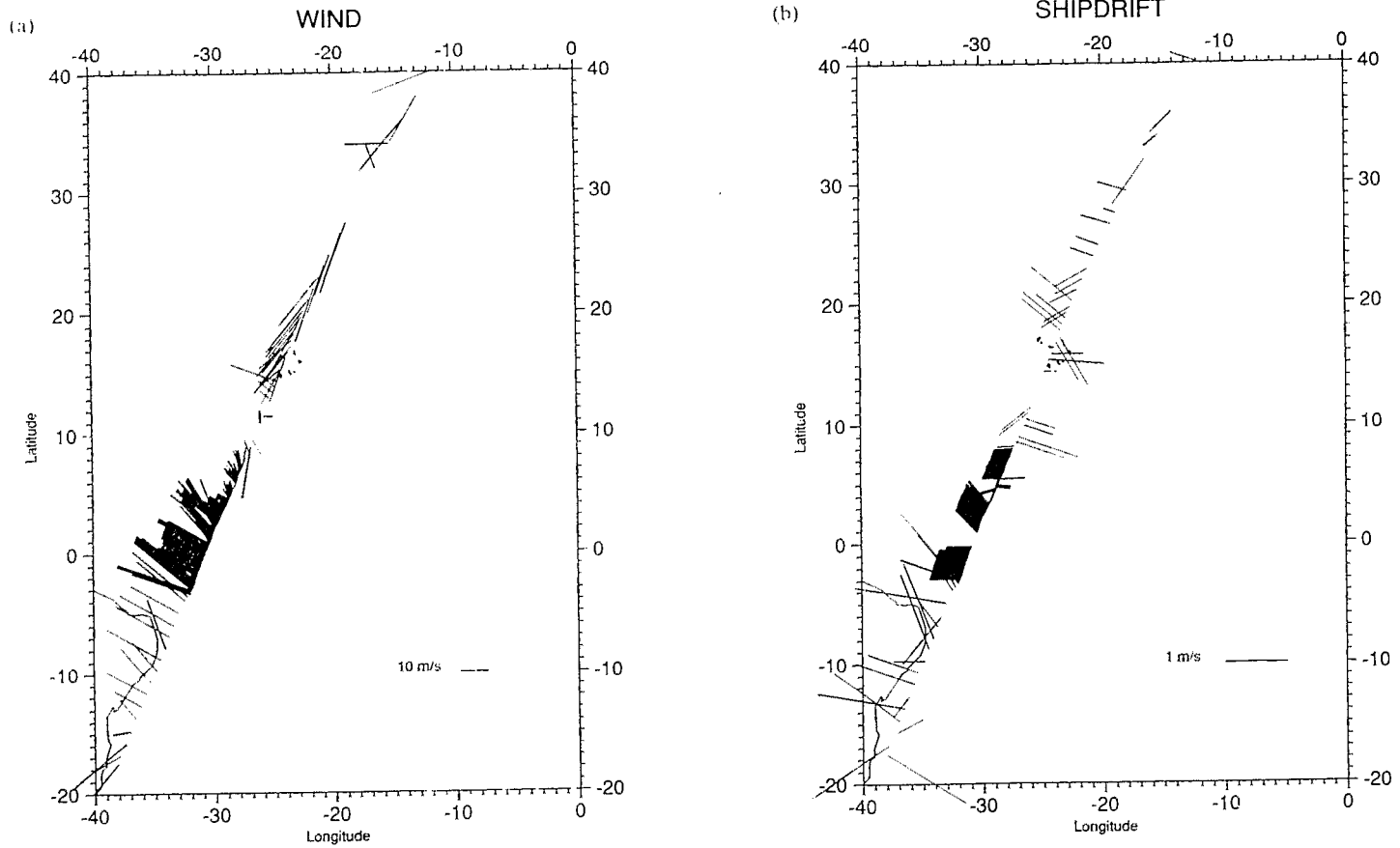
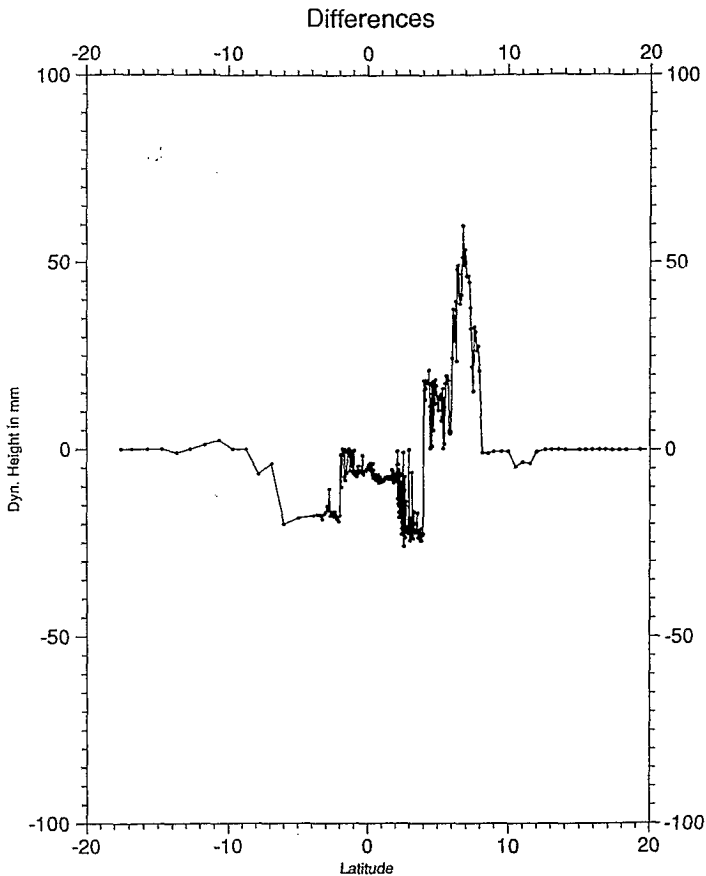Fig. 4. Surface wind (a) and drift (b) along the shiptrack as observed during the cruise. Unit is m s^{-1}.

Fig. 5.   Difference between dynamic heights computed without a *T–S* correction applied at the surface and with a *T–S* correction applied at the surface. Unit is dyn mm.

winds and currents at that time (Fig. 4a and b). These surface temperature and salinity anomalies created local dynamic heights effects as large as 8 cm (Fig. 5). Therefore, it was important to take into account these effects before computing the DHA for the cruise, as we explained in Section 3.

The agreement between the SLA for the track 104, which follows the shiptrack, and the DHA (Fig. 6) is particularly good north of the equator:

— positive extremum (+10 cm) at 16°N,
— negative extremum (−12 cm) at 12°N in the North Equatorial Current region,
— positive extremum (+10 cm) at 7–8°N,
— negative extremum (−4 to −5 cm) at 3°N at the southern edge of the North Equatorial Counter Current which weakens at that time in 88,
— positive extremum (+10 cm) at 1–2°S in the South Equatorial Current.

The correlation between the SLA and the DHA (Table 1) is better in the northern hemisphere and can reach 0.75 between 5°N and 15°N. The mean rms is between 4 and 6 cm. In the southern hemisphere, south of 5°S, the negative correlation (−0.23) indicates an out-of-phase variation of the DHA and the SLA.

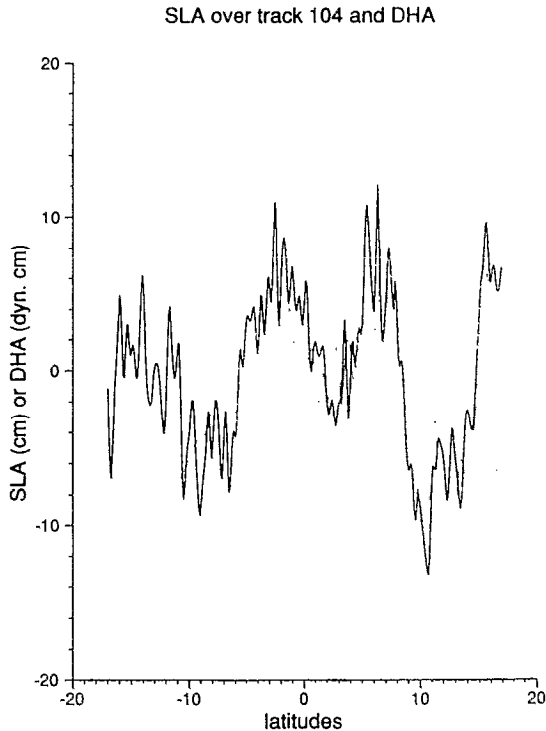SLA over track 104 and DHA

Fig. 6.   Comparison of Dynamic Height Anomalies (DHA in dyn cm) along the shiptrack and Sea Level Anomalies (SLA in cm) for track 104. Dashed line is for DHA and continued line is for SLA.

We also performed a spectral analysis on the data sets. Both power spectra present similar energy levels (Figs 7 and 8), with a k^{-1} dependence from 100 to 1000 km as observed by Fu (1983) for low energetic regions. A linear adjustment gives a $k^{-1.3}$ dependence for SLA and $k^{-1.5}$ for DHA between 100 and 1000 km. The cut-off occurs around 70 km for DHA: it occurs around 50 km for SLA and is more evident than for the DHA. This is probably explained by the initial different sampling of the data.

Although the ship took an entire week to travel along the line, the GEOSAT flew over it in only 8 min on 2 October. To avoid problems due to time and space high variability, we therefore computed from the altimetric data set a new satellite derived track collocated in both time and space with the ship locations. This was done through an objective analysis (DE MEY and ROBINSON, 1987). We used 48 tracks over the 20°N–20°S × 20°W–40°W

Table 1.   *Correlation coefficients and mean rms between the DHA and SLA in the southern, the equatorial and the northern parts of the shiptrack*

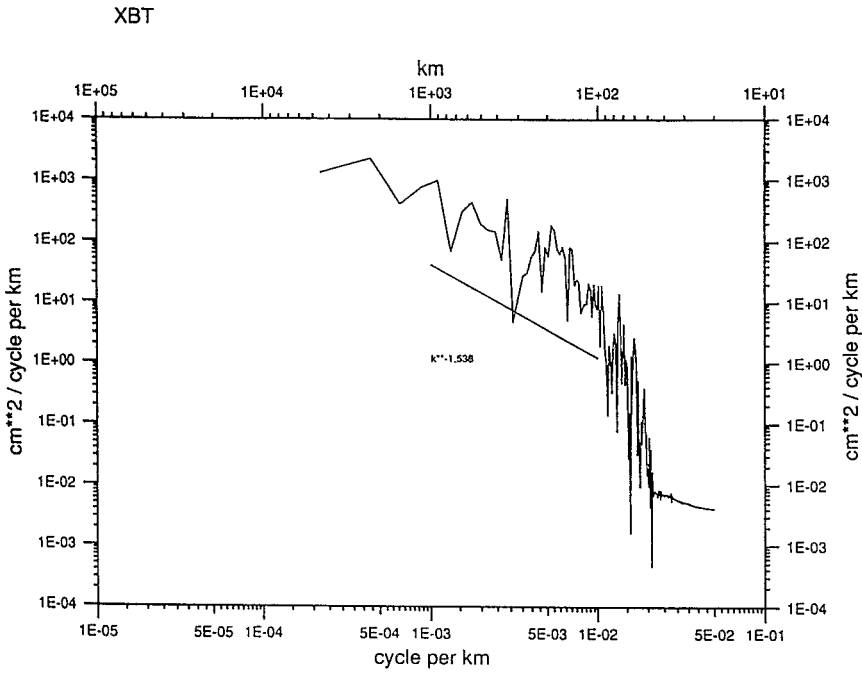| Region	rms (cm)	r	[r1, r2]
15°S– 5°S	6.4	−0.23	−0.37, −0.52
5°S– 5°N	4.4	0.11	−0.06, 0.27
5°N–15°N	4.7	0.75	0.66, 0.81

XBT

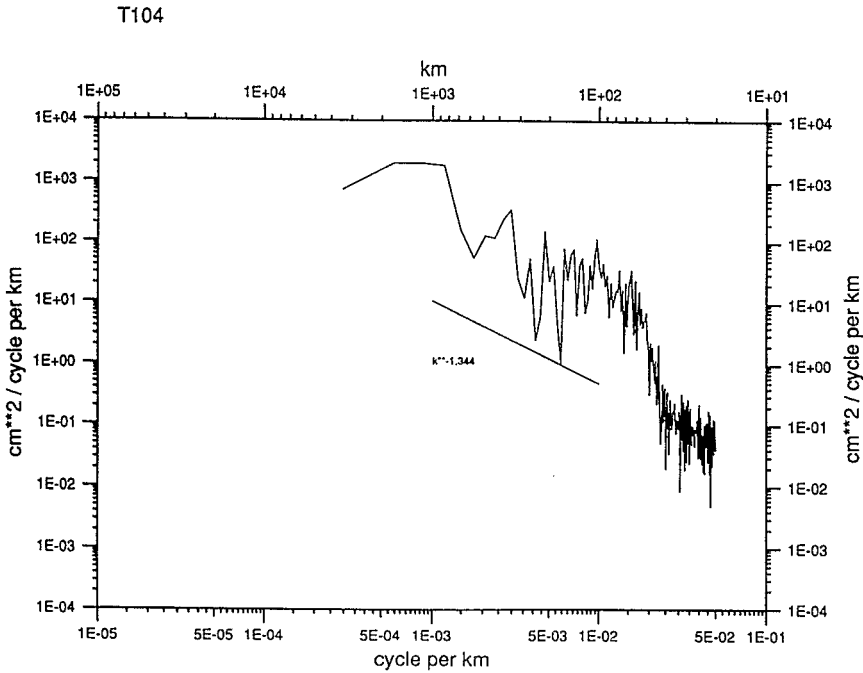Fig. 7. Power spectrum for the DHA.

T104

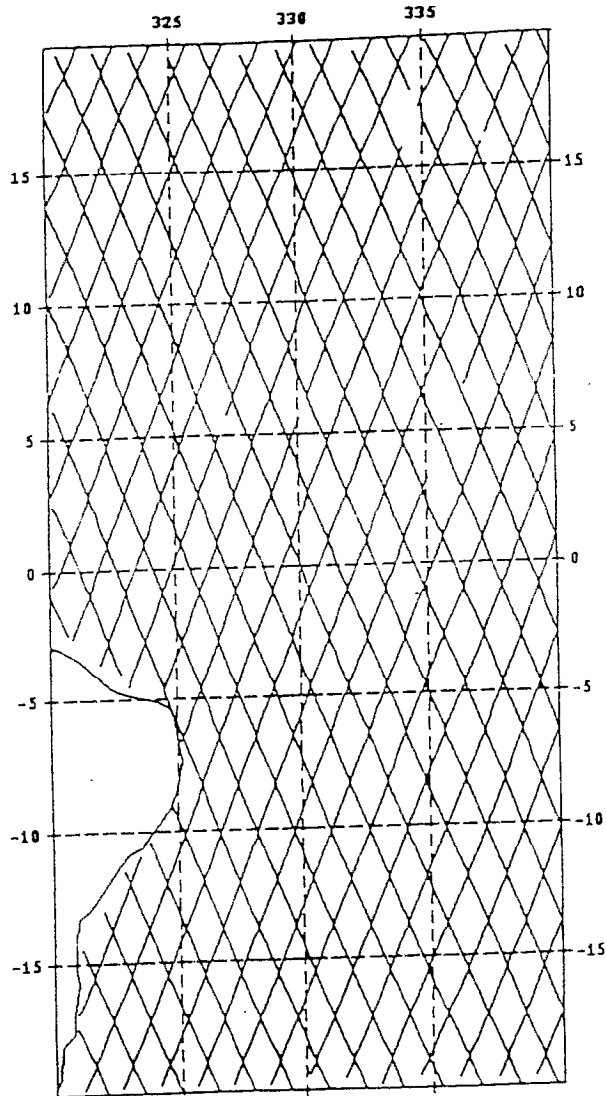Fig. 8. Power spectrum for the SLA along track 104.

Fig. 9.   GEOSAT tracks used in the objective analysis.

region (Fig. 9). The spatial decorrelation scale given by DHA autocorrelation function (Fig. 10) along the shiptrack is 500 km, in good agreement with earlier studies. Based on these indications, we selected the decorrelation scales for the objective analysis at 600 km in longitude, 400 km in latitude and 10 days in time. The search radii were chosen at, respectively, 700 and 500 km and 15 days. The correlation function was:

$$f = (1 + K^*R^*(1 - (K^*R)^2/3))^* \exp(-K^*R)^* \exp(-T) \quad \text{with K constant} = 2.103803$$

$$R = ((dx/rx)^2 + (dy/ry)^2)^{1/2}, \quad rx, ry \text{ spatial decorrelation scales}$$

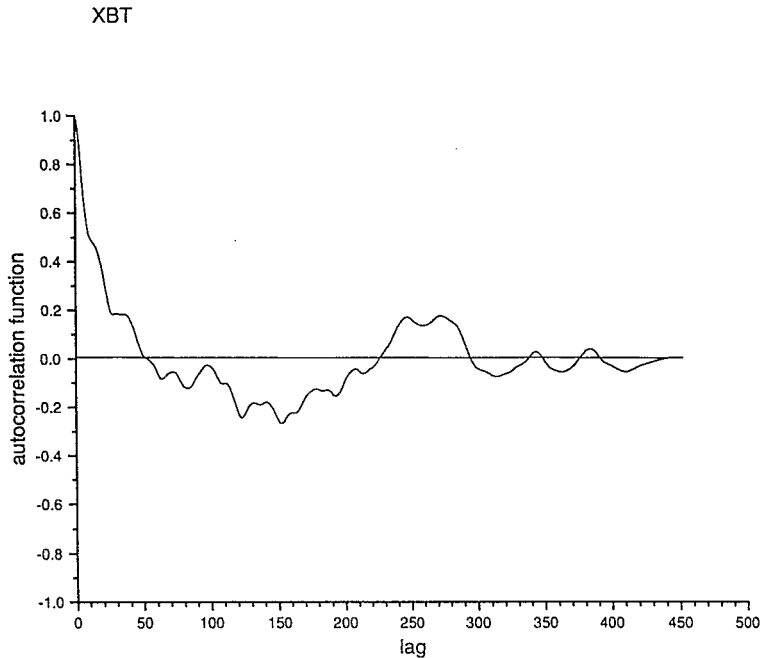$$T = dt^2/rt^2, \quad rt \text{ temporal decorrelation scale.}$$

XBT

Fig. 10.   Autocorrelation function of the DHA along the shiptrack. Units for the lag corresponds
to 10 km.

The mesh size was 0.5° in longitude and latitude. Figure 11 presents this new recomposed ship co-located SLA together with DHA. All the structures already depicted by Fig. 6 are still evidenced except that the troughs at 3 and 12°N are less pronounced. The very high spatial variability has been removed from the original SLA through the objective analysis. The correlation between this new SLA and DHA has significantly increased in all the regions (Table 2) to reach more than 0.87 in the northern hemisphere with a mean rms around 4 cm, which is rather similar to those observed using tide-gauges in the Pacific (TAI *et al.*, 1989; CHENEY *et al.*, 1989). At large wavelengths, the power spectrum (Fig. 12) presents the same energy level as the XBTs (Fig. 7), but due to high variability smoothing operated by the analysis (the smallest decorrelation scale is 400 km), the cut off around 70 km is not so clear and the k^{-1} dependence has changed to k^{-3} for the wave numbers less than 200 km.

5. DISCUSSION

This comparison demonstrates the good agreement that exists between *in situ* data and altimetry, especially north of the Equator. We focus now the discussion on the differences encountered south of 5°S.

Several explanations, such as different dynamical processes, correction residual errors and sampling effects, could be formulated.

As noted in Section 3, altimetric measurements are subject to many sources of error. The wet tropospheric error correction, as given in the GDRs (CHENEY *et al.*, 1987) is

problematic because of the uncertainty in the FNOC model fields. This correction is critical in the tropics, especially along the mean position of the InterTropical Convergence Zone (ITCZ). We did not produce complete meteorological soundings during the campaign for measuring the integrated water vapour. But during the cruise we collected, information concerning the saturation vapour pressure (Fig. 13) and cloudiness indexes (Fig. 14). Both figures indicate a maximum activity located north of 5°N, but not south of 5°S. Thus. it is clear that the wet tropospheric correction is not mainly responsible for the SLA/DHA disagreement south of 5°S. On the other hand. the good SLA/DHA agreement encountered between 5°N and 20°N, where the tropospheric correction also seems to be important, confirms that this long wavelength error—even if not perfectly corrected by FNOC model—is reasonably filtered out by the altimetric data processing. Ionospheric correction is not considered as a major problem because our study was conducted during a period of relatively low solar activity. Thus, it was lower than during the SEASAT mission where it was already not very significant (LORELL *et al.*, 1982). The barotropic effects become important near the coasts. as along the American coast where the oceanic tides have larger amplitude. Barotropic tide effects are removed from altimetric data using SCHWIDERSKI's model (1980), but as noticed earlier errors of several centimetres can persist. Nevertheless, it seems that. if tide corrections appear to be important off the mouth of the Amazon river, further south, they are not so large (C. LE PROVOST and P. VINCENT. personal communication). Thus tide effects cannot explain the whole part of the
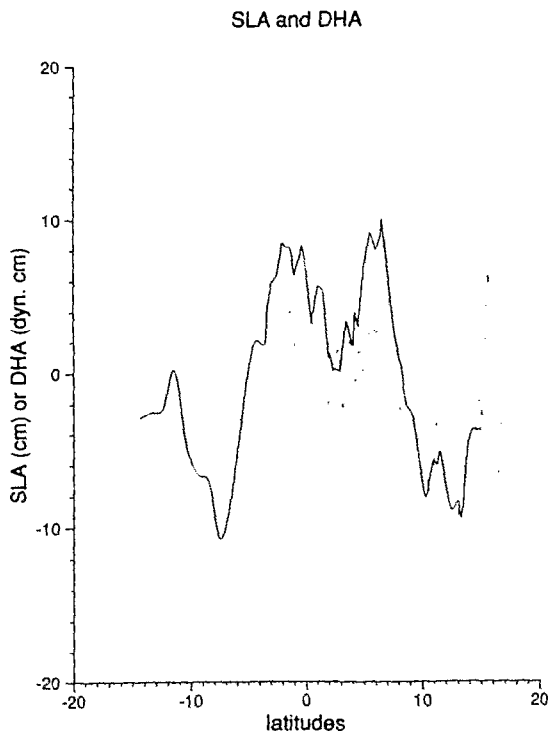
SLA and DHA

Fig. 11. Comparison of Dynamic Height Anomalies (DHA in dyn cm) along the shiptrack and Sea Level Anomalies (SLA in cm) for the concomitant track recomposed through an objective analysis. Dashed line is for DHA and continued line is for SLA.

Table 2.   *Correlation coefficients and mean rms between
the DHA and SLA in the southern, the equatorial and the
northern parts of the shiptrack, after an objective analysis
on the altimetric data*

Region	rms (cm)	r	[r1, r2]
15°S– 5°S	5.8	−0.08	−0.28, −0.73
5°S– 5°N	4.8	0.57	0.44, 0.67
5°N–15°N	3.8	0.88	0.83, 0.91

difference encountered between SLA and DHA south of 5°S, when both the shiptrack and the satellite track skim the coast. We also investigated the possible contribution of residual orbit error first by looking at a longer track (30°N–30°S instead of 20°N–20°S) and by applying a second degree polynom fit. The results are rather similar to those presented in Fig. 6 and Table 1. The mean rms and the correlation coefficient south of 5°S are 5.5 cm and −0.29, respectively. We also used the new available GEMT2 orbit, but the results in the south remain the same: rms = 5.5 cm r = −0.24. Thus, residual orbit errors do not seem to significantly contribute to the observed discrepancies.

Another possible explanation for the discrepancy between the two data sets in the South Atlantic, could come from the importance of the salinity correction when computing *in situ*
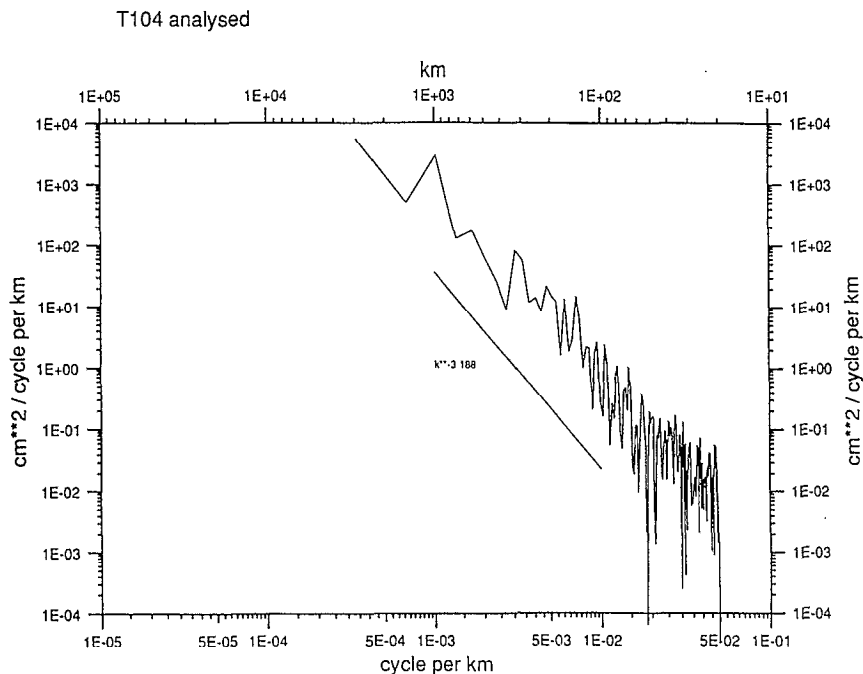

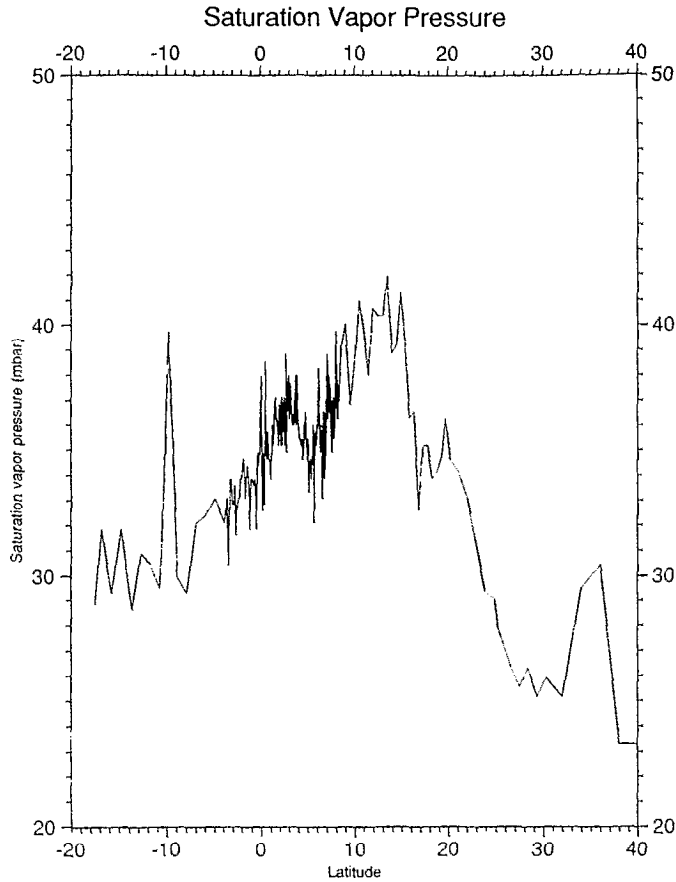Fig. 12.   Power spectrum for the recomposed SLA.

Saturation Vapor Pressure

Fig. 13   Saturation vapor pressure along the shiptrack observed during the cruise. Unit is mbar.

surface dynamic heights. But as revealed by Fig. 3. this correction only plays a key role near 7°N. Elsewhere, the temperature and salinity samples taken during the cruise are very similar to the historical surface temperatures and salinities and consequently do not introduce significant differences in the dynamic height calculation.

We remind the reader that altimetry refers to the entire column of water when the DHA are referenced to 500 m depth and therefore only provides information about the baroclinic surface layers. During the FOCAL/SEQUAL experiment in 1982–1984, the comparison between 0/500 dbar dynamic heights computed from hydrographic stations. tide gauges records and inverted echo-sounders (KATZ et al., 1986; GARZOLI. 1987; HISARD and HÉNIN, 1987) demonstrated that the tropical Atlantic is mostly baroclinic for the first orders. This has been confirmed by numerical experiments (PHILANDER and PACANOSKI, 1981: DU PENHOAT and TRÉGUIER, 1985; DU PENHOAT and GOURIOU, 1987). But near the South American coast, CURTIS (1984) observed that isotherms between 20 and 10°C diverge at 11°15′S. This divergence is consistent with southward flow at the surface adjacent to Brazil and with northward flow of intermediate waters at depth. It occurs around 36°W which is near the GEOSAT track and the shiptrack (Fig. 1). so that it could
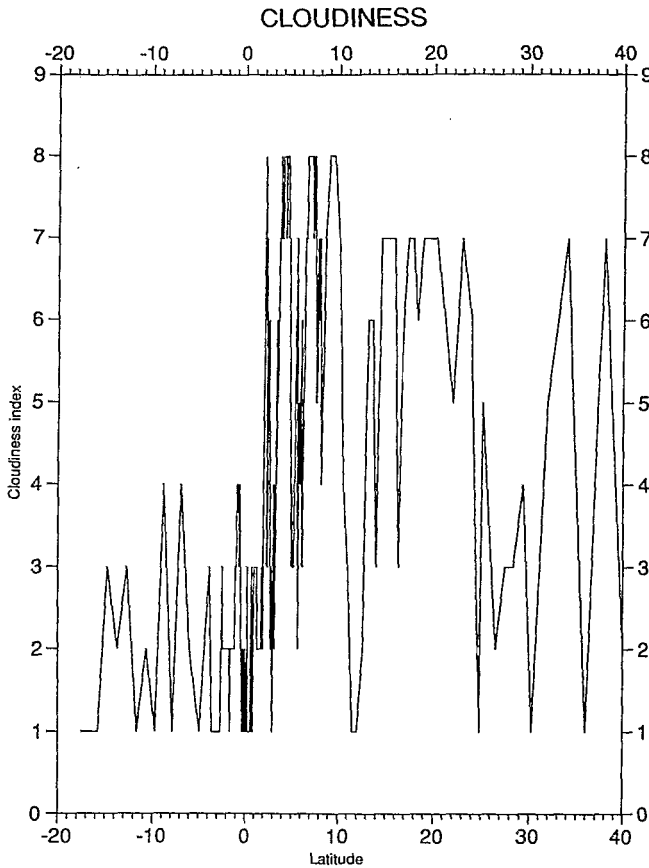
Fig. 14.   Cloudiness index along the shiptrack observed during the cruise.

be possible that altimetry and XBTs have sampled different oceanic phenomena with respect to the depth of reference.

CURTIS (1984) also observed several dips revealing mesoscale activity. Measuring the time-variability of the surface currents by the eddy kinetic energy derived from ship drift, RICHARDSON and McKEE (1984) showed a broad maximum with values greater than 400 cm^2 s^{-2} in energy between approximately 10°S and 10°N, and that along the south Brazilian coast values can reach more than 1200 cm^2 s^{-2}. There is no doubt therefore that this region near the coast is affected by small scale processes (eddy structures) and boundaries currents that present high variability in space and time (Fig. 4b). This is confirmed by the results of a three-dimensional model of the tropical Atlantic forced with monthly 86–88 winds (MORLIÈRE, personal communication). It is interesting to see that the correlation with GEOSAT track 190 (just to the east of track 104), closer in time with the · XBTs measurements in this part of the shiptrack (10/05/1988), is 0.5 with a mean rms equal to 4.3 cm. It is also noteworthy that ship drift observed during the cruise (Fig. 4b) does not present any coherence south of 5°S as they do along the northern part of the line. Therefore, non-synoptic data with a different grid spacing can sample different structures.

These are the most plausible explanation for the DHA/SLA differences in the southern hemisphere.

REFERENCES

Arnault S., Y. Ménard and J. Merle (1990) Observing the tropical Atlantic ocean in 86–87 from altimetry. *Journal of Geophysical Research*, **95**, 17,921–17,945.

Bernstein R. L., G. H. Born and R. H. Whritner (1982) SEASAT altimeter determination of ocean current variability. *Journal of Geophysical Research*, **87**, 3261–3268.

Cartwright D. E. and R. J. Taylor (1971) New computations of the tide generating potential. *Geophysical Journal of the Royal Society*, **23**, 45–74.

Cartwright D. E. and A. C. Edden (1973) Corrected tables of tidal harmonics. *Geophysical Journal of the Royal Society*, **23**, 253–264.

Cheney R. E. and J. G. Marsh (1981) SEASAT altimeter observations of dynamic topography in the western north Atlantic. *Journal of Geophysical Research*, **86**, 473–483.

Cheney R. E., J. G. Marsh and B. D. Beckley (1983) Global mesoscale variability from collinear tracks of SEASAT altimeter data. *Journal of Geophysical Research*, **88**, 4343–4354.

Cheney R. E., B. C. Douglas, R. W. Agreen, L. L. Miller and D. L. Porter (1987) *GEOSAT altimeter Geophysical Data Record (GDR) user handbook.* National Ocean Survey/NOAA, 23 pp.

Cheney R. E., B. C. Douglas and L. Miller (1989) Evaluation of GEOSAT altimeter data with application to tropical Pacific sea level variability. *Journal of Geophysical Research*, **94**, C4, 4737–4747.

Curtis A. C. (1984) A trans-Atlantic upper-ocean temperature section along 11°15'S in March 1983. *Geophysical Research Letters*, **11**, 773–774.

Daniault N. and Y. Ménard (1985) A comparison of eddy kinetic energy distribution in the Southern Ocean from SEASAT altimeter and FGGE free drifting buoys. *Journal of Geophysical Research*, **90**, 11877–11890.

De Mey P. and A. R. Robinson (1987) Simulation and assimilation of satellite altimeter data at the oceanic mesoscale. *Journal of Physical Oceanography*, **17**, 2280–2293.

Dessier A. and J. R. Donguy (1991) Sea surface salinity in the tropical Atlantic ocean (10°S–30°N)—Seasonal and interannual variability (1977–1986). In preparation.

Du Penhoat Y. and A. M. Tréguier (1985) The seasonal linear response of the tropical Atlantic Ocean. *Journal of Physical Oceanography*, **15**, 316–329.

Du Penhoat Y. and Y. Gouriou (1987) Hindcasts of equatorial sea surface dynamic height in the atlantic in 82–84. *Journal of Geophysical Research*, **92**, 3729–3740.

Emery W. J. (1975) Dynamic height from temperature profiles. *Journal of Physical Oceanography*, **5**, 369–375.

Emery W. J. and R. T. Wert (1976) Temperature–salinity curves in the Pacific and their application to dynamic height computation. *Journal of Physical Oceanography*, **6**, 613–616.

Emery W., G. H. Born, D. Baldwin and C. Norris (1990) Satellite derived water vapor corrections for GEOSAT altimetry. *Journal of Geophysical Research*, **95**, 2953–2964.

Fu L. (1983) On the wave number spectrum of oceanic mesoscale variability observed by SEASAT altimeter. *Journal of Geophysical Research*, **88**, 4331–4342.

Fu L. and D. B. Chelton (1985) Observing large scale temporal variability of ocean currents by satellite altimetry: with application to the Antarctic Circumpolar Current. *Journal of Geophysical Research*, **90**, 4721–4739.

Garzoli S. (1987) Forced oscillations on the equatorial Atlantic. *Journal of Geophysical Research*, **92**, 5089–5100.

HASTENRATH S. (1982) On meridional heat transport in the world ocean. *Journal of Physical Oceanography*, **12**, 922–927.

HISARD P. and C. HÉNIN (1987) Response of the equatorial Atlantic ocean to the 1983–1984 wind from the Programme Français Océan et Climat dans l'Atlantique equatorial, cruise data set. *Journal of Geophysical Research*, **92**, 3759–3768.

JOURDAN D., C. BOISSIER, A. BRAUN and J. F. MINSTER (1990) Influence of wet tropospheric correction on mesoscale dynamic topography as derived from satellite altimetry. *Journal of Geophysical Research*, **95**, 17, 993–18, 004.

KATZ E. J., P. HISARD, J. M. VERSTRAETE and S. L. GARZOLI (1986) Annual change of the sea surface slope along the Equator of the Atlantic ocean in 1983–1984. *Nature*, **322**, 245–247.

KOSRO P. M., P. FLAMENT and A. HUYER (1988) *A comparison between relative surface topography from altimetry and from the hydrography during CTZ*. Coastal Transition Zone Newsletter 3(2), Woods Hole Oceanographic Institute, Woods Hole, Massachusetts.

LORELL J., E. COLQUITT and R. J. ANDERLE (1982) Ionospheric correction for SEASAT altimeter height measurement. *Journal of Geophysical Research*, **87**, 3207–312.

MALARDE J. P., P. DE MEY, C. PERIGAUD and J. F. MINSTER (1987) Observation of long equatorial waves in the Pacific Ocean by Seasat altimetry. *Journal of Physical Oceanography*, **17**, 2273–2279.

MARSH J. G. and T. V. MARTIN (1982) The SEASAT altimeter mean sea surface model. *Journal of Geophysical Research*, **87**, 3269–3280.

MÉNARD Y. (1983) Observation of eddy fields in the northwest Atlantic and the northwest Pacific by Seasat altimeter data. *Journal of Geophysical Research*, **88**, 1853–1866.

MÉNARD Y. (1988) Observing the seasonal variability in the tropical Atlantic from altimetry. *Journal of Geophysical Research*, **93**, 13,967–13,978.

MERLE J. and S. ARNAULT (1985) Seasonal variability of the surface dynamic topography in the tropical Atlantic Ocean. *Journal of Marine Research*, **43**, 267–288.

MILLER L., R. E. CHENEY and D. MILBERT (1986) Sea level time series in the equatorial Pacific from satellite altimetry. *Geophysical Research Letters*, **13**, 475–478.

MONALDO F. (1990) Path length caused by atmospheric water vapor and their effects on the measurement of mesoscale ocean circulation features by a radar altimeter. *Journal of Geophysical Research*, **95**, 2923–2932.

MUSMAN S. (1986) Sea slope changes associated with westward propagation equatorial temperature fluctuations. *Journal of Geophysical Research*, **91**, 10,753–10,757.

PHILANDER S. G. H. and R. C. PACANOWSKI (1981) Response of equatorial oceans to periodic forcing. *Journal of Geophysical Research*, **86**, 1903–1926.

RICHARDSON P. and T. MCKEE (1984) Average seasonal variation of the Atlantic Equatorial currents from historical ship drifts. *Journal of Physical Oceanography*, **14**, 1226–1238.

SAASTAMOINEN J. (1972) *Atmospheric correction for the tropospheric and stratospheric in radio ranging of satellites*. Geophysical Monograph, 15, American Geophysical Union, Washington, DC.

SCHWIDERSKI E. W. (1980) On charting global tides. *Review of Geophysical Space Physics*, **18**, 243–268.

STOMMEL H. S. (1947) Note on the use of T–S correlation for dynamic height anomaly computation. *Journal of Marine Research*, **5**, 85–92.

TAI C. K., W. B. WHITE and S. E. PAZN (1989) GEOSAT cross over analysis in the tropical Pacific. 2, verification analysis of altimetric sea level maps with expendable bathythermograph and island sea level data. *Journal of Geophysical Research*, **94**, 897–908.

TAPLEY B. D., J. B. LUNDBERG and G. H. BORN (1982) The Seasat altimeter wet tropospheric range correction. *Journal of Geophysical Research*, **87**, 3213–3220.